Simultaneous Improvement to Signal Integrity and Electromagnetic Interference in High-Speed Transmission Lines

Towards Realization of Branched Traces for High-Speed Data Transfer in PCBs

Moritoshi Yasunaga, Yusuke Kuribara, Hirofumi Inoue
Graduate School of Systems and Information Engineering
University of Tsukuba
Tsukuba, Ibaraki 305-8573, JAPAN
yasunaga@cs.tsukuba.ac.j

Ikuo Yoshihara
Faculty of Engineering
Miyazaki University
Gakuen Kibanadai Nishi, Miyazaki 889-2192, JAPAN

***Abstract*—Branched traces are strictly prohibited in the routing of printed circuit boards (PCBs) for high-speed data transfer, because they cause serious degradation of the signal integrity (SI) and excessive electromagnetic interference (EMI). If this strong design constraint can be removed, the number of degrees of freedom increases dramatically, and the operation speed in PCBs is expected to be improved significantly. In an attempt to overcome the SI degradation that occurs due to characteristic impedance mismatching, we previously proposed the bio-inspired segmental transmission line (STL), and we demonstrated its effectiveness. In this paper, we apply the STL to a branched trace for high-speed data transfer, and we use genetic algorithms to try to simultaneously improve its SI and EMI. Some branched STL prototypes are fabricated and evaluated; the results, which include eye diagrams and electromagnetic emission intensities, show a big improvement in SI and EMI in branched traces.**

I. Introduction

With the advent of the GHz era, the electrical wavelengths of digital signals propagating in printed circuit board (PCB) traces have become shorter, and they are now about the same length as the traces. As a result, the traces for high-speed signals (e.g., clock-signal distribution networks, data/address-busses, and I/O links) must be designed as transmission lines, because slight mismatches in the characteristic impedances of the traces can cause the reflection of waves, which leads to data transfer errors. Fig. 1 shows an example of a waveform observed in a double data rate (DDR) memory bus trace operating at 1 GHz; note that the waveform is seriously distorted by reflection waves due to the characteristic impedance mismatching. Conventional designs for matching characteristic impedances [1][2], however, do not work well in the GHz domain (more precisely, from about 500 MHz), and new techniques to counteract the waveform distortion have been urgently desired.

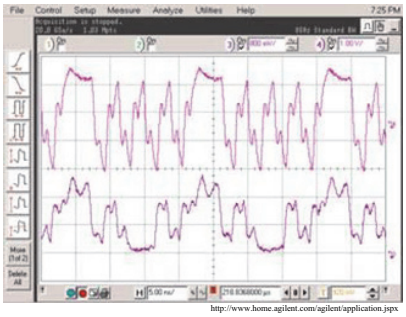

http://www.home.agilent.com/agilent/application.jspx

Fig. 1 Measured waveform in a DDR memory bus

This signal integrity (SI) degradation is now a serious problem in PCBs but not yet in large-scale integrated circuits (LSIs). However, it is expected to become a problem in LSIs in the near future, because when the operating frequency exceeds 10 GHz, the electrical wavelength (λ) of the digital signals become about the same length (*l*) as the connections in the LSIs (Fig. 2).

In order to overcome the SI degradation problem in the GHz domain, we previously proposed a novel trace structure called the segmental transmission line (STL); its bio-inspired design methodology uses genetic algorithms (GAs) [3]. We demonstrated its effectiveness by applying it to various real high-speed links, including memory bus systems and backplane bus systems [4]. In these bus systems, *stub* traces (Fig. 3(a)), which are very short branches, are used to connect devices (e.g., LSIs and memory modules) to the main trace. The stub and the device cause the mismatching of the characteristic impedances, and this results in degradation of the SI. Our previous applications of STLs to real bus systems clearly demonstrated that the STL is very effective for real link structures that consist of a main bus with stubs and devices.

978-1-4799-7560-0/15 $31.00 © 2015 IEEE
DOI 10.1109/SSCI.2015.177

A *branched* trace (Fig. 3(b)) or bifurcated trace is used to split the main trace so that signals are distributed to other routing paths; this has the same topology as that of the stub trace shown in Fig. 3. However, stubs and branched traces are completely different in terms of SI degradation and electromagnetic interference (EMI). Stub traces are short enough that they can be regarded electrically as a load capacitance that is a lump component. No electromagnetic waves (and thus no EMI) is emitted at the stub, because compared with the electromagnetic waves, the stub is short enough that it cannot become an emission *antenna*.

In comparison to a stub trace, a branched trace is much longer, and its length is generally comparable to that of the main trace, and thus it behaves as a transmission line instead of a lumped load capacitance. Consequently, in addition to the characteristic impedance mismatching, multiple reflections, which cause serious SI degradation, occur in the branched trace. As a result, fatal SI degradations frequently arise.

Furthermore, the branched trace, which has almost the same length as that of the propagation signal, behaves as an antenna and emits electromagnetic waves; if multiple reflections occur, it creates EMI. Strong EMI affects not only the LSIs mounted on the same PCB, but also those on other PCBs, and it causes them to malfunction. The amount of EMI is thus restricted under electromagnetic compatibility (EMC) regulations, which are defined in each region or country; in Japan, these are the Voluntary Control Council for Interference by Information Technology Equipment (VCCI) regulations.

Because of the serious SI degradation and strong EMI, branched traces are strictly prohibited in the trace-routing for high-speed data transfer, and this constraint has greatly impeded the design of trace routes. If both of these serious difficulties can be overcome simultaneously, and the prohibition is lifted for using branched traces for high-speed digital signals, the flexibility of routing designs will increase significantly, and the system performance will improve dramatically.

In this paper, we take on the difficult challenge of simultaneously increasing SI and reducing EMI in branched traces; we do this by applying the STL, which leads to multiobjective optimization of the SI and EMI. Our goal is to remove the restrictions on the use of branched traces in the GHz era.

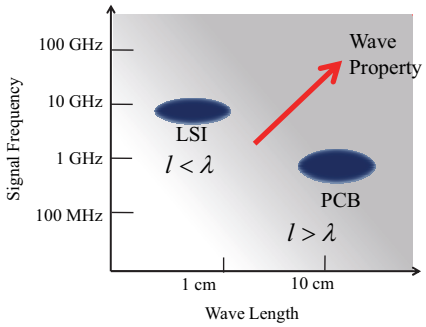

Fig. 2 Relationship between electrical wavelength and signal frequency

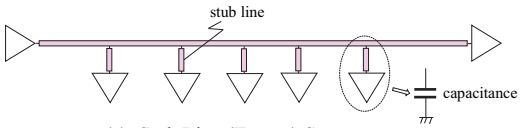

(a) Stub Line (Trance) System

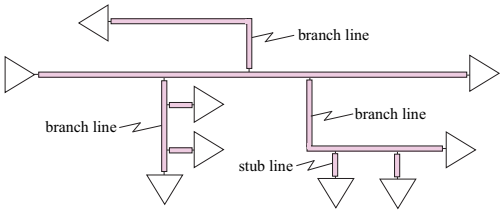

(b) Branch and Stub Line (Trance) System

Fig. 3 Stub and branched trace

II. Basic Idea of STL

In the STL, a transmission line is divided into multiple (N) segments, each with their own individual characteristic impedance Z_i (i = 1, 2, ..., N), as shown in Fig. 4 [3][4]. The values of Z_i in the various segments are adjusted to achieve an ideal digital waveform at important points, such as the input points, by superposing the reflection waves that are generated at the interface between adjacent segments Z_i and Z_j. Fig. 4 shows an elevated view of a PCB trace that is designed as an STL: the characteristic impedance Z_i is a function of the trace width W_i, so Z_i is adjusted by adjusting W_i.

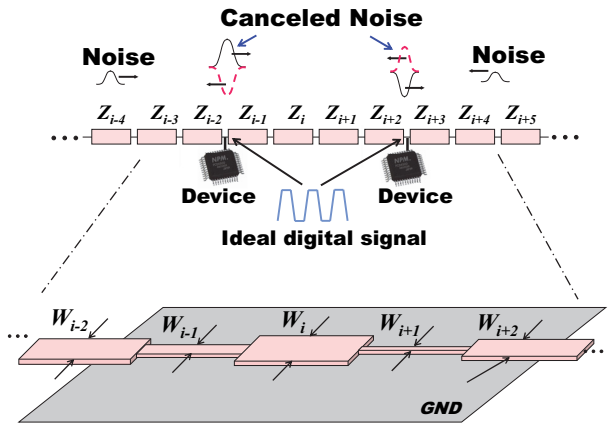

Fig. 4 Basic idea of the STL and its application to a PCB trace

The adjustment of all of the Z_is, however, results in a combinatorial explosion: for example, if there are 10 segments ($N = 10$) and 100 characteristic impedance candidates (from 21 Ω to 120 Ω at intervals of 1 Ω), the resulting search space reaches 100^{10}, and there is no deterministic search algorithm that can find the optimized or semi-optimized set of Z_is. We thus proposed applying genetic algorithms (GAs) as a way to manage this combinatorial explosion. The STL structure can be easily mapped onto a one-dimensional array of parameters, as shown in the upper section of Fig. 5 (here, the transmission line is divided into 10 segments).

In an earlier design, we used only the characteristic impedances Z_i as genes in a *simple chromosome* (see the upper example in Fig. 5). As a modification of this early design, we proposed a *hybrid chromosome*, which was created by adding segments of length L_i as genes (see the lower example in Fig. 5). The segment lengths L_i can adjust the timing of the superposition of the reflected waves, and thus we expect that the hybrid chromosomes result in greater SI than that obtained from the simple chromosomes.

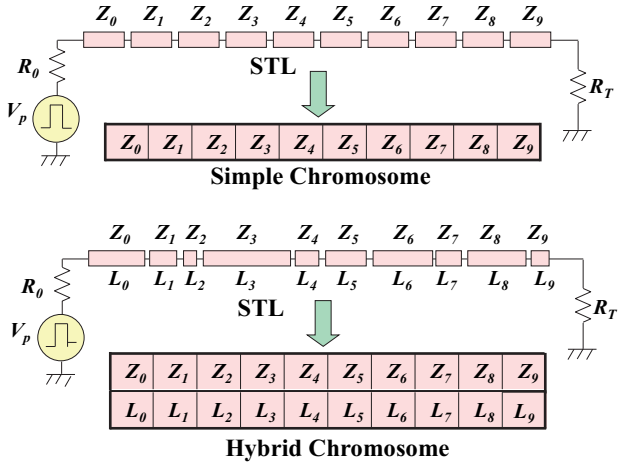

Fig. 5 Simple chromosome (upper) and hybrid chromosome (lower)

III. Design Methodology Based on Genetic Algorithms

A. Fundamental GA operations

Initially, characteristic impedances are given randomly to all the genes in a set of chromosomes or a population, as shown in Fig. 6. After the population is generated, the three operations of selection, crossover, and mutation are then applied to the population, and this process is repeated until the fitness (the score of the chromosome) is significantly improved.

The waveform of each chromosome is simulated using a SPICE circuit simulator, as shown in Fig. 6. Each chromosome is scored according to the difference *Diff* between the area of the ideal waveform $I(t)$ and that of the distorted waveform $R(t)$, as shown in Fig. 7. For periodic or clock signals, the reciprocal of *Diff* is used as the score (fitness), so that the score increases as the waveform is improved or as it approaches the ideal waveform.

In a crossover, randomly selected pairs of chromosomes exchange parts of their genes at randomly chosen crossover points. In a mutation, some randomly chosen genes are changed to other values; this occurs with a rather low probability.

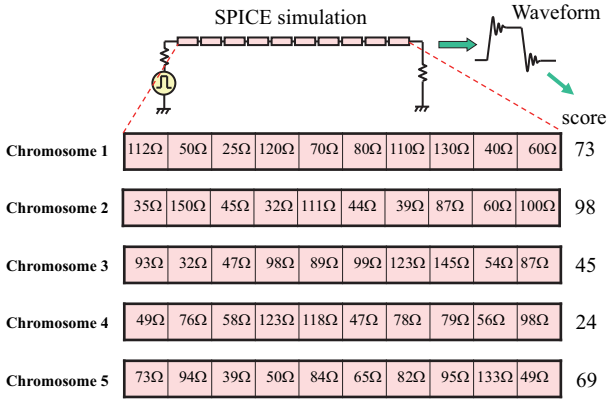

Fig. 6 A population and evaluation of its chromosome

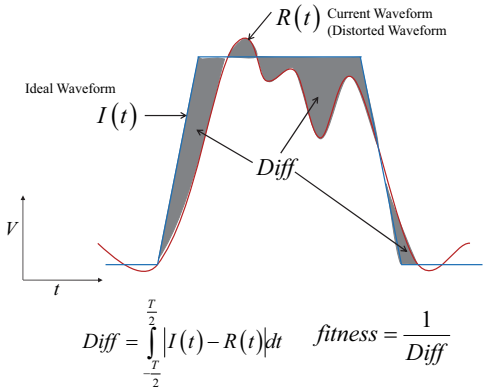

Fig. 7 Fitness of a periodic signal

B. *Modified Crossover*

The crossover operation is the key to successful evolution in the STL design, and so we have changed the simple crossover operation to the minimal generation gap (MGG) algorithm [5], which is a well-known genetic algorithm that was initially proposed to ensure a diverse population. In the MGG algorithm, parents are randomly selected from individuals in the *N*-th generation, and their children are generated by crossover operations, as shown in Fig. 8. From each family, one chromosome is selected (based on quality or chance), and it is exchanged with one chromosome in the *N*-th generation to produce the *N*+1-st generation. Since the waveform is very sensitive to the characteristic impedance and the segment length of the STL, as the population evolves, it generally becomes less diverse. We thus use the MGG algorithm to avoid the loss of diversity when designing an STL.

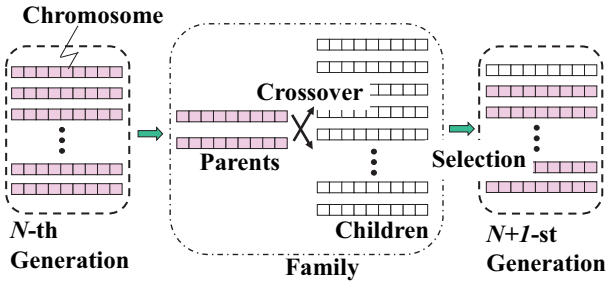

Fig. 8 Crossover in the minimal generation gap algorithm used with the STL

It has been shown that, in the STL design, intervals of 1 Ω are sufficiently small that the Z_i can be treated as integers. Within each segment, the Z_i are mutually independent, and thus fatal genes cannot be generated by the simple crossover operation. In a simple chromosome or the Z_i part of a hybrid chromosome, genes can be easily exchanged by a simple crossover operation.

On the other hand, the crossover operation for the segment length L_i is not as easy as it is for the Z_i, because there is a strict condition that the sum of all segment lengths L_i is fixed as the trace length. Furthermore, the timing of the superposition of the waveforms is very sensitive to the propagation time. We thus have to treat the L_i as real number genes with a fixed trace length.

Fig. 9 shows a newly proposed crossover operation for the L_i genes; it is based on the BX-α crossover [6][7]. For example, a 20 cm trace is divided into 5 segments, and before the crossover operation, the segment lengths L_i are normalized and changed to the boundaries A1 to A4 in chromosome 1 and to B1 to B4 in chromosome 2. We then choose at random two boundaries, say, A3 and B3, that have no other boundaries between them. The range B3 to A3 is then expanded by α percent ($10 \le \alpha \le 20$). Finally, two new boundaries, A3* and B3*, are chosen randomly from the expanded range, and their lengths are changed. This expanded BX-α crossover has worked well in practical applications and has found excellent solutions for the design of STLs.

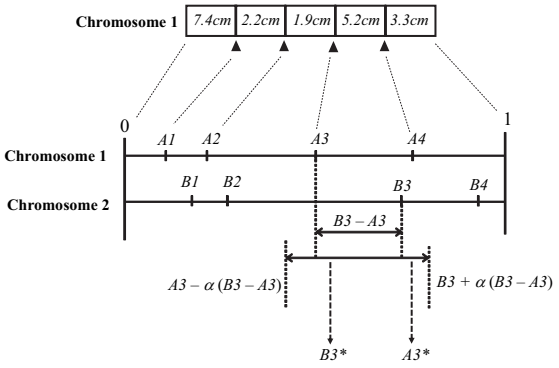

Fig. 9 BX-α crossover for a hybrid chromosome

C. *Fitness for Random Signal (Data Signal)*

For periodical signals, the fitness (score) is calculated directly from its waveform, as described above (Fig. 7). For random signals, however, we cannot use the same measure of fitness, since by definition, they are not periodic. In order to overcome this difficulty, we use impulse response theory: If the ideal impulse propagates in the trace, impulse response theory guarantees high SI. Therefore, we use an impulse, or a long periodic signal of 1000000…1000000… as shown in Fig. 10, and the difference *Diff* between the area of the ideal impulse waveform $I(t)$ and that of its response waveform $R(t)$ is used as the fitness (score). Again, the fitness increases as the response waveform improves and approaches the ideal impulse, and the reciprocal of *Diff* is defined as the fitness.

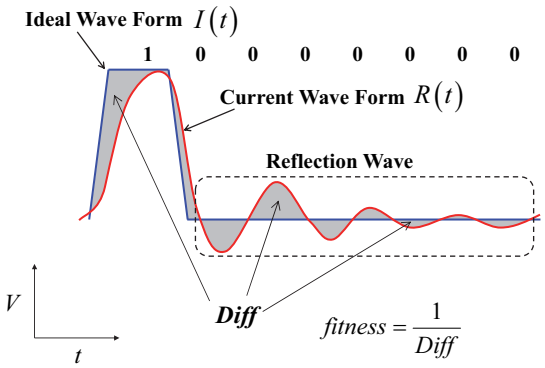

Fig. 10 Fitness of random signals

IV. Simultaneous Improvement of SI and EMI

In addition to improving the SI, we wish to simultaneously reduce the EMI in the branched traces. In order to meet this requirement, we extend the fitness function based on the multiobjective optimization approach by adding a measure of EMI fitness to the measure of SI fitness. In the EMI evaluation, we use the Japanese EMI regulations (VCCI standards), in

which the emission limit is defined for both the MHz and GHz frequency domains, as shown in Fig. 11.

To extend the measure of fitness, we simply sum the emissions that exceed the VCCI limit (Fig. 11), and we then use the reciprocal of this as the new measure of fitness. We then add the emission fitness $fitness_{EMI}$ to the SI fitness $fitness_{SI}$, defined above, as follows:

$$fitness = \alpha\,(fitness_{SI} / fitness_{SI\_50\Omega}) + \beta\,(fitness_{EMI} / fitnesse_{EMI\_50\Omega}) \quad (1)$$

where α and β are weighting parameters; and $fitness_{SI}$ and $fitness_{EMI}$ are normalized by $fitness_{SI\_50\Omega}$ and $fitness_{EMI\_50\Omega}$, respectively, which are their values in a conventional 50Ω transmission line (this is done because $fitness_{SI}$ and $fitness_{EMI}$ have different units). This measure of fitness, based on multiobjective optimization, works very well, and its effectiveness will be demonstrated below when evaluating the prototype.

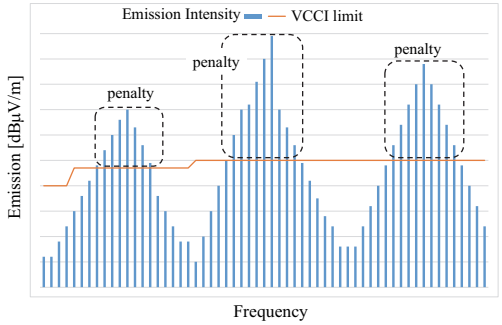

Fig. 11 EMI regulations (VCCI) and the EMI score

V. Prototype Design and Evaluation

A. Prototype of a branched trace

Scaled-up prototypes, in which the lengths of the transmission lines and the load capacitances are enlarged in proportion to the ratio of the frequencies, are frequently used to evaluate GHz waveforms in the MHz domain, especially if there is a possibility that the measurement equipment will affect the GHz waveforms. Such a scaled-up prototype for branched trace routing is shown in Fig. 12; in the 250 MHz (500 Mbps) STL scaled-up prototype for a trace length of 1 GHz (2 Gbps), the trace length and the load capacitor were designed to be 60 cm and 7 pF, respectively, with a scale-up ratio of 4 (the ratio of 250 MHz to 1 GHz). The prototype consists of a 60 cm main trace and two 22 cm branch traces, each end of which has a load capacitance equivalent to the input capacitance of a device.

In the STL design, each branched trace (transmission line) was divided into 5 segments (for a total of 10 segments). This seemed to be an appropriate number of segments, based on the target frequency. Currently, however, no deterministic design principle has yet been established for the number of segments. We thus carried out some preliminary simulations in which the number of segments was varied between 10 and 20, and we determined that 10 segments was sufficient.

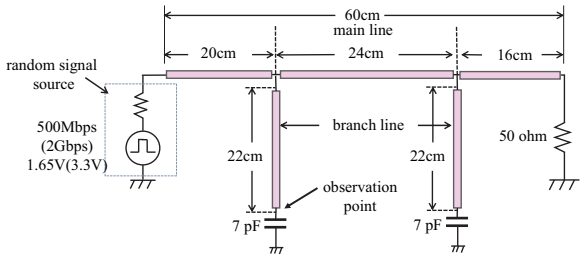

Characteristic impedances of main line and branch lines are all designed to be 50 Ω.

Fig. 12 Branched trace for scaled-up prototype at 1 GHz

B. Simultaneous Improvement to SI and EMI in the Prototype

We have designed several STLs in which we changed the values of the weighting parameters α and β in Eq. (1), and the resulting EMI charts are shown in Figs. 13–17, in which the emission intensity is calculated at each frequency as follows:

$$E = (E_h^2 + E_v^2)^{1/2}, \quad (2)$$

where E_h and E_v are the horizontal and vertical emission components, respectively.

Fig. 13 shows the EMI for a simulation in which the EMI fitness was not added to the SI fitness (e.g., $\alpha = 1$ and $\beta = 0$). Some strong emission spectra that exceeded the VCCI limit were observed in the GHz range; this would affect the LSIs mounted not only on the same PCB but also those mounted on other PCBs.

On the other hand, as shown in Fig. 14, those strong emission spectra are greatly suppressed when design of the STL considers only improvement of the EMI (e.g., $\alpha = 0$ and $\beta = 1$). Although there are still a very few emissions that exceed the limit in the GHz range, they are small enough that it is thought they will not affect the surrounding LSIs.

The EMI obtained under the equal weighting design (e.g., $\alpha = 0.5$ and $\beta = 0.5$) is shown in Fig. 15. A strong emission spectrum (over 60 dBμV/m) still remains at around 1.25 GHz. This spectrum is not reduced even with $\alpha = 0.33$ and $\beta = 0.67$ (Fig. 16), but it is reduced to approximately the limit when $\alpha = 0.25$ and $\beta = 0.75$ (Fig. 17). Because of this, for the design of a prototype for practical use, we chose $\alpha = 0.25$ and $\beta = 0.75$.

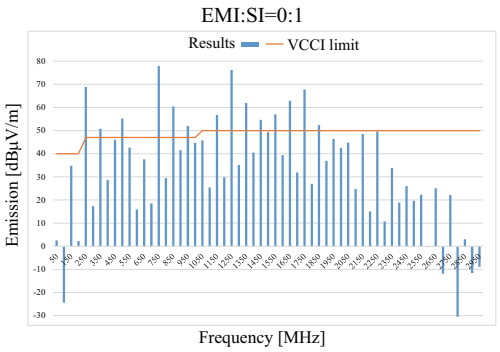

Fig. 13 EMI when $\alpha = 1$ and $\beta = 0$

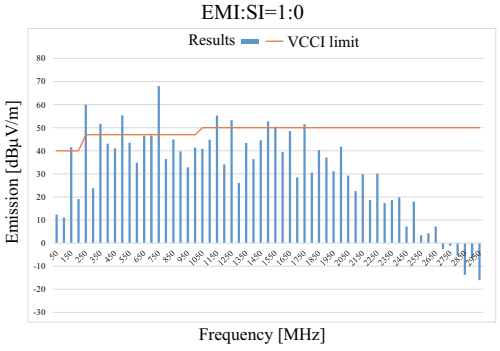

Fig. 14 EMI when $\alpha = 0$ and $\beta = 1$

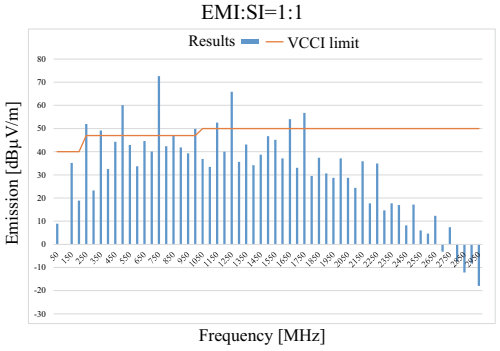

Fig. 15 EMI when $\alpha = 0.5$ and $\beta = 0.5$

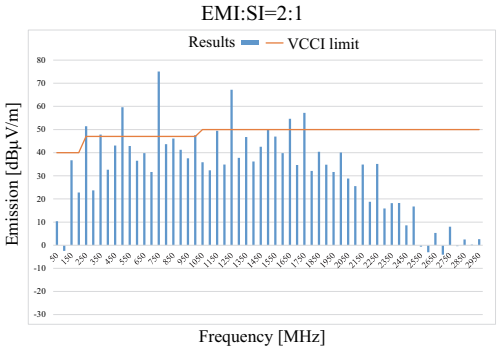

Fig. 16 EMI when $\alpha = 0.33$ and $\beta = 0.67$

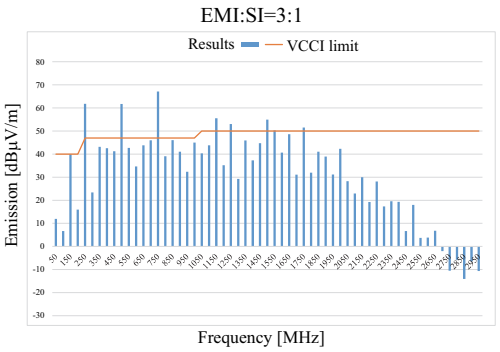

Fig. 17 EMI when $\alpha = 0.25$ and $\beta = 0.75$

C. Impulse Response under EMI constraint

Simulation results for the impulse response in the conventional 50 Ω characteristic impedance (Fig. 12) are shown in Fig. 18. An impulse with a voltage of 1.5 V and a width of 2 ns was input, and the response was observed at the end of the left branch of the trace. The response was very different from the initial impulse. In the response, the input impulse is deformed, and the amplitudes of the oscillations exceed the voltage of the initial impulse; the first and second amplitudes are 3.36 V and 1.86 V, respectively. This is due to the multiple reflections at the observation point. These oscillations continue for about 30 ns, which is more than seven times the clock period. This large distortion greatly increases the intersymbol interference (ISI) and can produce fatal errors in digital systems.

Fig. 19 shows the resulting design for this STL. In the chart in the lower panel, the vertical and horizontal axes shows each segment's characteristic impedance and length, respectively (the impedance and length of the main trace are also shown). It is notable that the characteristic impedances of the segments on the left side branch, where the observation point is located, are all a bit smaller than 50 Ω (the characteristic impedance of the conventional trace), while those on the right side branch are all much larger than 50 Ω. This seems to occur because the waveform in a branched trace is strongly affected not only by that trace but also by the trace in the other branch.

Fig. 20 shows the improved response of this STL (Fig. 19). The severely distorted impulse response that was shown in Fig. 18 is greatly improved in this STL: the large first and second oscillations that were seen in Fig. 18 are now suppressed to 2.22 V and 0.591 V, respectively, and the oscillations converge within 20 ns. From the improved response, the ISI is expected to be suppressed enough for practical use, and thus the SI in the random signal is expected to be greatly improved.

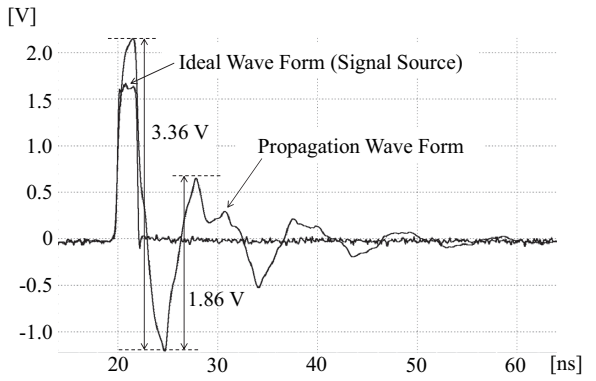

Fig. 18 Impulse response in conventional 50 Ω transmission line (trace)

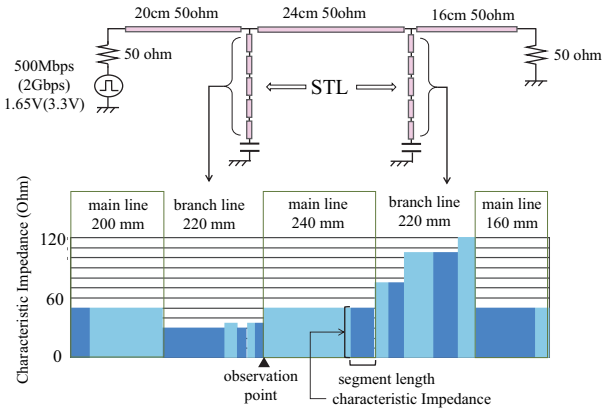

Fig. 19 Results for new STL design

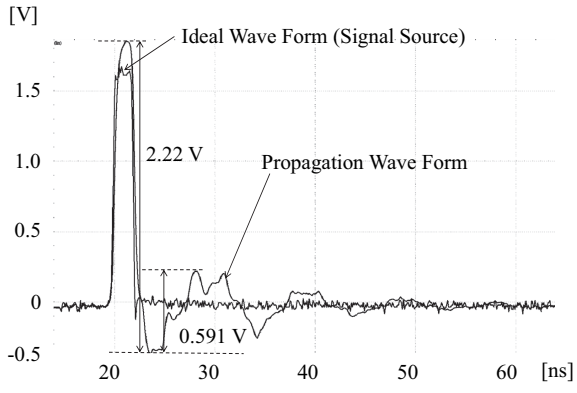

Fig. 20 Impulse response in the STL

D. Measured Results

Photographs of the fabricated 250 MHz scaled-up prototypes based on the resulting STL design (Fig. 19) and the conventional trace design (Fig. 12) are shown in Fig. 21. The lower photograph in Fig. 21 shows the STL scaled-up prototype, and the upper one shows a conventional trace (transmission line) with a uniform characteristic impedance of 50 Ω. The STL and the conventional transmission line both run for a total of 40 cm with a U-turn, and the space between the lines is designed to be sufficiently wide to prevent crosstalk noise. Chip capacitors (load capacitances) of 7 pF were connected to each end of the branch trace; these represent the input capacitances of devices, such as LSIs. When observing the waveform, we used a digital-storage oscilloscope with a 2 GHz bandwidth and a 10 GS/s sampling rate (WR204Xi, LeCroy Ltd.).

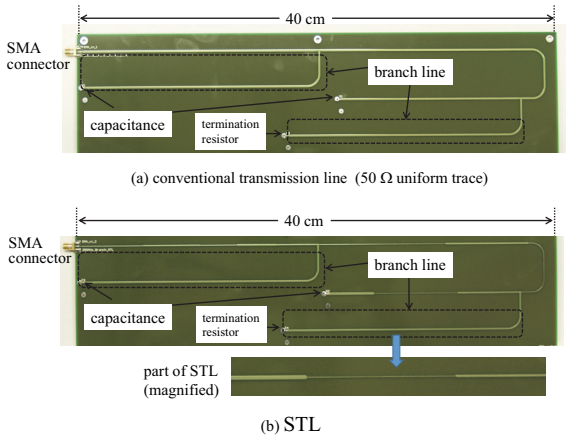

Fig. 21 Branched trace prototype

An *eye diagram*, in which a random digital signal sequence has been repeatedly sampled at the data rate, is generally used to measure the interference in a random signal, and the left and right panels in Fig. 22 show those observed in the conventional transmission line and in the STL, respectively.

As anticipated, the eye diagram for the conventional trace is severely distorted due to the large oscillations in the response (as shown in Fig. 18), and so no aperture is observed in the eye diagram. This result clearly shows the well-known fact that a branched trace is not appropriate for high-speed data links. In contrast to that of the conventional transmission line, the eye diagram in the STL clearly opens to a height of 1.01 V and a width of 1.66 ns, which is sufficiently large to be used in practice.

We have designed and fabricated some other STL prototypes for different branch lengths. Fig. 23 shows the eye diagrams for STLs designed for 12 cm and 32 cm branched traces. In these cases, the apertures clearly open to almost the same degree as those shown in Fig. 22. Those results demonstrate the high adaptability and generality of the STL design methodology for branched traces.

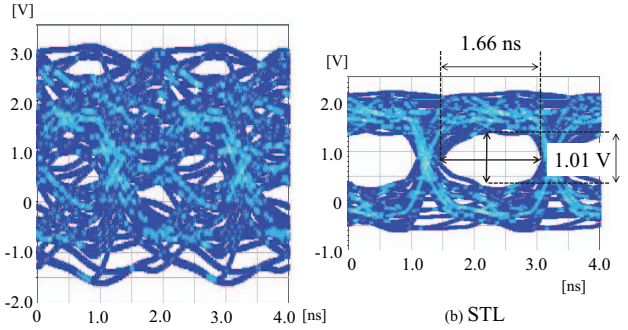

(a) conventional transmission line (50 ohm uniform trace)

Fig. 22 Eye diagrams for branched trace prototypes

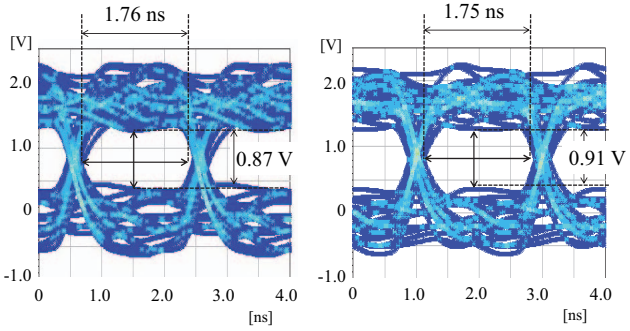

12 cm branch line 32 cm branch line

Fig. 23 Eye diagrams for the STL (12 cm and 32 cm branch traces)

We measured the electromagnetic emissions of the prototype inside of a certified electromagnetic shielded room. Figs. 24 and 25 show the measured E_h and E_v, respectively; these are as defined in Eq. (2). Unfortunately, due to the limitations of the instruments, we were not able to measure emissions above 1 GHz.

Under 1 GHz, the measured emissions are slightly less than those for the simulation shown in Fig. 17, and a possible reason for this is that the electrical loss in the trace suppresses the emissions from the trace, and this loss was higher in the prototype than in the simulation. We are planning to measure the EMI in the GHz range, and it is expected that the measured emissions will be less than those shown in Fig. 17.

VI. Conclusions

The use of branched traces are strictly prohibited for high-speed data transfer in PCBs, due to degradation of the SI and to excessive EMI. In order to simultaneously improve the integrity and reduce the interference, we applied an STL to the branched trace. The STLs were designed using a multiobjective measure of fitness for the SI and EMI. Prototypes were fabricated for some systems with different branched traces. In all cases, the SI was improved, and their EMI was suppressed to within the limits of the VCCI regulations.

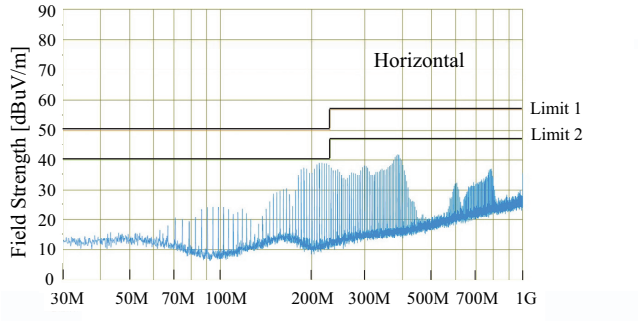

Fig. 24 Measured EMI in the horizontal component

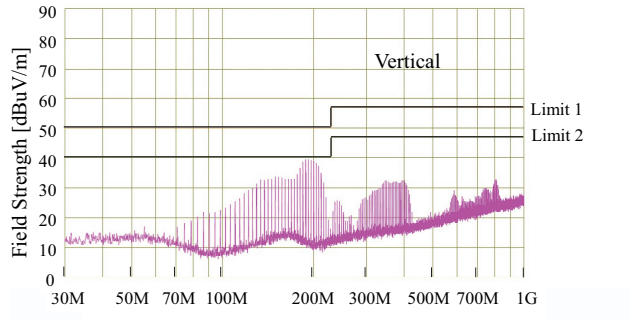

Fig. 25 Measured EMI in the vertical component

Acknowledgments

This research was partially supported by the Japan Society for the Promotion of Science (JSPS) KAKENHI grant number 26289114.

References

[1] Eric Bogatin, Signal and Power Integrity: Simplified, 2nd ed., Prentice Hall Signal Integrity Library, 2010.

[2] Mike Peng Li, Jitter, Noise, and Signal Integrity at High-Speed, 1st ed., Prentice Hall Signal Integrity Library, 2007.

[3] Moritoshi Yasunaga, Yoshiki Yamaguchi, Hiroshi Nakayama, Ikuo Yoshihara, Naoki Koizumi, and Jung H. Kim, "The Segmental-Transmission-Line: Its Design and Prototype Evaluation," Proc. The 8th International Conference on Evolvable Systems (Springer, Lecture Notes in Computer Science 5216, G. S. Hornby, L. Sekanina, P. C. Haddow Eds.), pp. 130-140, Prague, Czech Republic, Sept. 2008.

[4] Moritoshi Yasunaga, Hiroki Shimada, Katsuyuki Seki, and Ikuo Yoshihara, "The Segmental-Transmission-Line: Its Application," Proc. International Conference on Evolvable Systems, pp. 23-30, Florida USA, Dec. 2014.

[5] H. Sato, I. Ono, and S. Kobayashi, "A new generation alternation model of genetic algorithms and its assessment," J. of Japanese Society for Artificial Intelligence, 12(5), pp. 734-744, 1997.

[6] L.J. Eshelman and J.D. Schaffer, "Real-Coded Genetic Algorithms and Interval-Schemata," Foundations of Genetic Algorithms 2, pp. 187-202, 1993.

[7] L.J. Eshelman, K.E. Mathias, and J.D. Schaffer, "Crossover Operator Biases: Exploiting the PopulationDistribution," Proc. ICGA97, pp. 354-361, 1997.